Available online at www.sciencedirect.com

ScienceDirect

IFAC PapersOnLine 55-41 (2022) 95–100

Co-Adaptive Myoelectric Interface for Continuous Control ⋆

Maneeshika M. Madduri * **Momona Yamagami** *
Augusto X. T. Millevolte * **Si Jia Li** **
Sasha N. Burckhardt *** **Samuel A. Burden** *
Amy L. Orsborn *,**

* *University of Washington, Department of Electrical & Computer Engineering, Seattle, WA 98195 USA.*
** *University of Washington, Department of Bioengineering, Seattle, WA 98195 USA.*
*** *University of Washington, Department of Neuroscience, Seattle, WA 98195 USA.*

Abstract: Neural interfaces provide novel opportunities for augmenting human capabilities in domains like human-machine interaction, brain-computer interfaces, and rehabilitation. However, the performance of these interfaces varies significantly across users. Decoders that adapt to individual users have the potential to reduce variability and improve performance but introduce a "two-learner" problem as the user simultaneously adapts to the changing decoder. We propose and experimentally test a game-theoretic framework to optimize closed-loop performance of a myoelectric interface for continuous control (based on surface electromyography, sEMG) through co-adaptation of the user and decoder. Human subjects learned to use our interface to perform a two-dimensional trajectory-tracking task. Closed-loop performance was affected by decoder learning rate but not by initialization or decoder cost weights. Our study indicates the potential for co-adaptation in humans and machines to optimize the performance of neural interfaces.

Keywords: human-in-the-loop systems, neural interfaces, sensorimotor control

1. INTRODUCTION

Direct control of devices using neural activity has many applications, including brain-computer interfaces to restore function (BCIs) (Carmena, 2013; Shanechi et al., 2017), human-machine interfaces (HMIs) (De Santis, 2021), rehabilitation (Reinkensmeyer et al., 2016; Li et al., 2016), neuroprosthetics (Hochberg et al., 2012), and augmenting human capabilities (Willett et al., 2021). However, variability in the efficacy of neural interfaces across users (Zhang et al., 2020) and variability in neural signals within a single user over time (Yamagami et al., 2018) present challenges to the safety and performance of these interfaces.

In such scenarios, interfaces that seamlessly adapt to users while also shaping how the user learns to control the interface are desirable. Such *co-adaptive* interfaces are more robust to variability across and within users by jointly optimizing the closed-loop interaction between the user and device. Previous studies explored how co-adaptation can reduce task error (Müller et al., 2017; Orsborn et al., 2014, 2012) and maximize interaction efficiency (De Santis, 2021). For example, Orsborn et al. (2014) proposes and validates *SmoothBatch*, a closed-loop adaptation algorithm that iteratively updates the decoder to reduce task error. However, algorithms that only consider error and ignore user effort lack theoretical guarantees of convergence.

Co-adaptive human-machine interfaces present a "two-learner" problem. Both the human and machine are learning in a closed-loop alongside each other. Game theory has been proposed in recent years as a framework to study two-learner dynamics in sensorimotor control (Braun et al., 2009; Li et al., 2019, 2016; Müller et al., 2017; Madduri et al., 2021). In particular, game theory provides techniques for predicting convergence to and stability of stationary points in two-learner systems (Ratliff et al., 2013; Başar and Olsder, 1999). Although *general-sum* games can arise in sensorimotor interactions (Braun et al., 2009), we contend that the special case of *potential games* (Monderer and Shapley, 1996), where the incentives of both learners are aligned, are particularly relevant in neural control applications. Prior studies have leveraged potential games to explore how human-decoder interactions co-adapt with practice, both in simulation (Madduri et al., 2021) and in human-subject experiments (Li et al., 2016, 2019). For example, (Li et al., 2019) modeled a robot and human physically interacting using game theory, and demonstrated that each learner estimating the other's controller will converge to the Nash equilibrium. Such two-learner models could predict and shape the evolution of user-decoder dynamics. However, predictions from the game-theoretic framework have not yet been experimentally tested for neural interfaces.

⋆ Funding: Meta Research; a National Science Foundation Graduate Research Fellowship to AXTM; and a National Defense Science and Engineering Graduate Fellowship Program to MMM.

10.1016/j.ifacol.2023.01.109

In this paper, we propose and experimentally test a game-theoretic framework to optimize closed-loop performance of a myoelectric interface (using surface electromyography, sEMG) through co-adaptation of the user and decoder. In particular, we model the user and decoder as two players in a potential game and implement a natural (co-)adaptation strategy for the decoder: iteratively update to minimize the decoder's cost. In a human subjects experiment with seven participants, we found that the user and decoder co-adapt to significantly improve tracking performance during a five-minute two-dimensional trajectory-tracking task. We explored three different decoder adaptation parameters: (1) decoder learning rate (i.e., rate of decoder adaptation), (2) decoder initialization, and (3) decoder cost weight (i.e., scaling of the decoder cost function). We found that decoder learning rate affected performance: the slower learning rate led to better tracking performance than the faster learning rate. We additionally found that decoder initialization location affected final decoder location but not task performance. Neither decoder initialization nor decoder cost weight affected task performance. Our findings indicate the potential for game-theoretic algorithms to optimize the performance of neural interfaces.

2. PROBLEM FORMULATION

We model the user and decoder as two players that interact in a closed-loop *dynamic game* (Başar and Olsder, 1999) wherein the user produces myoelectric signal $s(t) \in \mathbb{R}^N$ that the decoder transforms into cursor position $y(t) \in \mathbb{R}^2$ to track the target trajectory $\tau(t) \in \mathbb{R}^2$.

We use a velocity-based decoder,

$$v(t) = D \cdot s(t), \; y(t) = y(0) + \int_0^t v(\sigma)\, d\sigma, \tag{1}$$

where the matrix $D \in \mathbb{R}^{2\times N}$ is synthesized by minimizing a linear combination of two costs – task *error* and decoder *effort* – defined by

$$\text{error} = \|D \cdot s - (\dot{\tau} - \dot{y})\|_2^2\,, \; \text{effort} = \|D\|_F^2\,; \tag{2}$$

here $\dot{x}$ denotes the time derivative and $\|x\|_2$ denotes the 2-norm of signal $x : [0,t] \to \mathbb{R}^d$, and $\|M\|_F$ denotes the Frobenius norm of matrix $M \in \mathbb{R}^{m\times n}$. Minimizing *velocity error* (2) is a common objective for invasive BCI (Orsborn et al., 2014; Wodlinger et al., 2015); we additionally consider the decoder effort in (2) because our theoretical analysis suggests that it is necessary to ensure the co-adaptation game has well-defined stationary points (Madduri et al., 2021).

The linear combination of error and effort that defines decoder cost $c(D)$ is determined by weighting $\lambda > 0$ as

$$c(D) = \|D \cdot s - (\dot{\tau} - \dot{y})\|_2^2 + \lambda \|D\|_F^2\,. \tag{3}$$

Under the hypothesis that users also seek to optimize a linear combination of task error and user effort analogous to (2), the user and decoder play a *potential game* (Hespanha, 2017, Ch. 12) whose theoretical properties have been the subject of a previous study (Madduri et al., 2021).

3. EXPERIMENTAL METHODS

Human subjects participants gave their informed consent prior to experimentation, according to study procedures approved by the University of Washington's Institutional Review Board (IRB #STUDY00014060).

3.1 Task

Participants were tasked with producing myographic signals to control a cursor to follow a target trajectory on a 2-dimensional computer display (Fig. 1). Participants were instructed to keep their cursor as close to the target as possible at all times.

The target trajectory was generated as a sum of two sinusoids with frequencies 0.10 and 0.25 Hz in the horizontal direction and 0.15 and 0.35 Hz in the vertical direction; to reduce the predictability of the target trajectory, the phases of the sinusoids were selected uniformly at random at the beginning of each trial. The target and cursor positions were updated and displayed at 60 Hz.

3.2 Conditions

The role of (1) decoder learning rate, (2) decoder initialization, and (3) decoder cost weight on co-adaptive system performance was tested.

(1) two different decoder learning rates were tested: *slow* ($\alpha = 0.75$) and *fast* ($\alpha = 0.25$).
(2) two randomized initializations of the D decoder matrix were used: *positive* (matrix elements chosen uniformly at random in the range $[0, 10^{-2}]$) and *negative* (elements chosen uniformly at random in $[-10^{-2}, 0]$).
(3) two decoder cost weights were tested: *low* ($\lambda = 10^2$) and *high* ($\lambda = 10^3$).

All combinations of the 2 learning rates, 2 initializations, and 2 decoder cost weights were tested for a total of 8 different conditions (2 learning rates × 2 initializations × 2 decoder cost weights). Each trial was 5 minutes long. This block of 8 trials was repeated twice for each participant with a 5-minute break in between blocks, and the order of conditions was randomized within blocks.

3.3 Data Acquisition, Filtering, and Processing

EMG signals were obtained using a Quattrocento system (Bioelettronica, Italy). A 64-channel electrode array (4mm inter-electrode spacing, 5x13 electrode rectangular layout) was placed around the forearm to target recordings from the Extensor Carpi Radialis. Electrodes were placed on the dominant arm for each subject. Once placed, the electrode array was wrapped with Coban self-adherent wrap (3M, Saint Paul, Minnesota).

Raw EMG signals were obtained using Biolite Software (Bioelecttronica, Italy) at 2048 Hz on Differential Mode with the built-in low-pass filter of 130 Hz and a high-pass filter of 10 Hz. The EMG signals were then filtered by delinearizing two consecutive 50 ms time windows with no overlap, and then taking the average of the delinearized signal to be used as the user input s (Yamagami et al., 2020). EMG data were mapped to cursor position as in (1).

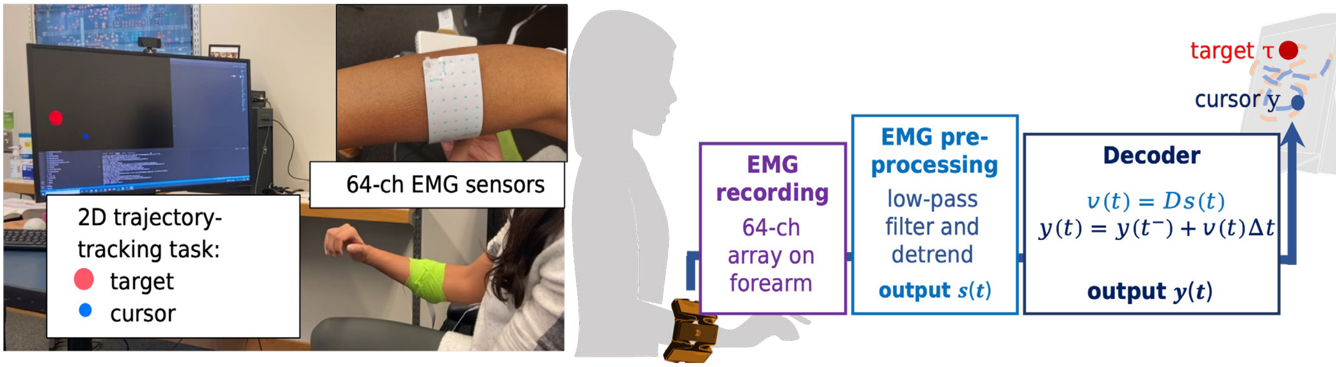

Fig. 1. (Left) The participant is tasked with following the red target by controlling the blue cursor. Participants controlled the blue cursor with the 64-channel Quattrocento EMG sensor on their forearm. (Right) Block diagram illustrating the transformation of myographic signals to the computer display.

3.4 Decoder Adaptation

Closed-loop decoder adaptation was performed to update the EMG-cursor movement transformation as the participant controlled the interface. Decoder adaptation used a supervised learning algorithm. The training signal is provided by inferring the user's intended velocity based on task goals, assuming that the user intends to move towards the provided target (Orsborn et al., 2012; Gilja et al., 2012). Decoder parameters were updated using a framework derived from the SmoothBatch algorithm (Orsborn et al., 2012). Rather than only task error, the cost function in (3), which combines *error* and *effort*, was minimized to determine optimal decoder parameters.

The decoder was updated iteratively using 20 second batches of data. Given a batch of data, the minimum D^* of the cost (3) was computed,

$$D^* = \min_D c(D), \tag{4}$$

and the updated decoder D^+ was determined using the SmoothBatch scheme (Orsborn et al., 2012), that is, by a convex combination of D and D^*,

$$D^+ = \alpha D + (1 - \alpha) D^*. \tag{5}$$

3.5 Data Analysis

Our primary metric for task performance was time-domain tracking error computed as the 2-norm between the target and cursor positions, $\|\tau - y\|_2$. For computing changes in task performance across the trial, we looked at relative error, $\frac{error_{fi}}{error_i} \times 100\%$, where error$_{fi}$ = error$_{final}$ - error$_{initial}$. We also compared the distance between final decoders of different initializations. To do so, we computed the average last final three decoders for each initialization (averaging across learning rates, blocks, and subjects), and then compared the distance between the initialization mean and each subject's initialization, $||D_{final,avg}$ - $D_{final,subj}||_F^2$.

The average performance of the *first* and *last* 20 seconds of the trial was used to compute the statistical significance of changes within trials. All analyses treat subjects as individual data points and take the median across other conditions (learning rate, initialization, decoder cost weight, and blocks). Statistical significance was assessed using the non-parametric Wilcoxon signed-rank tests.

4. EXPERIMENTAL RESULTS

A total of 7 people (3 women, 3 men, and 1 who declined to answer) participated in the study. Participants were primarily right-handed (6 right-hand, 1 left-hand; 57% all dominant, 29% mostly dominant, and 14% ambidextrous in handedness), with an average weight and standard deviation of 141 ± 19.3 lbs, a height of 66 ± 3.5 in, a forearm circumference of 9.6 ± 1.0 in and an age of 23 ± 3.0 years. All participants were daily computer users.

4.1 Co-Adaptation Improved Trajectory-Tracking

Task performance, as measured by time-domain tracking error, improved within individual trials (Fig. 2): comparing tracking error for the *first* to the *last* 20 seconds across all conditions (learning rate, initialization, decoder effort weight, and trial block), we found that performance significantly improved within trials (Fig. 3).

4.2 Decoder Learning Rate Affected Performance

The slow learning rate yielded better tracking performance (Fig. 4): comparing the relative error between the *first* and *last* 20 seconds, we found a significantly greater improvement in performance for the slow learning rate than for the fast learning rate (Fig. 5a).

4.3 Decoder Initialization Affected Final Decoder

Comparing the relative error of the *first* to the *last* 20 seconds between *positive* and *negative* decoder initializations, we found no significant impact on performance (Fig. 5b). Final task performance did not differ significantly between the two initializations. However, the final decoder solutions were influenced by initialization: the distance between final decoders was smaller within the same initialization than across initializations (Fig. 6).

4.4 Decoder Cost Weight Affected Decoder Effort

Comparing the relative error of the *first* to the *last* 20 seconds between the *high* and *low* decoder cost weights, we found no significant effect on task performance (Fig. 5c). However, we did observe an effect on the Frobenius norm

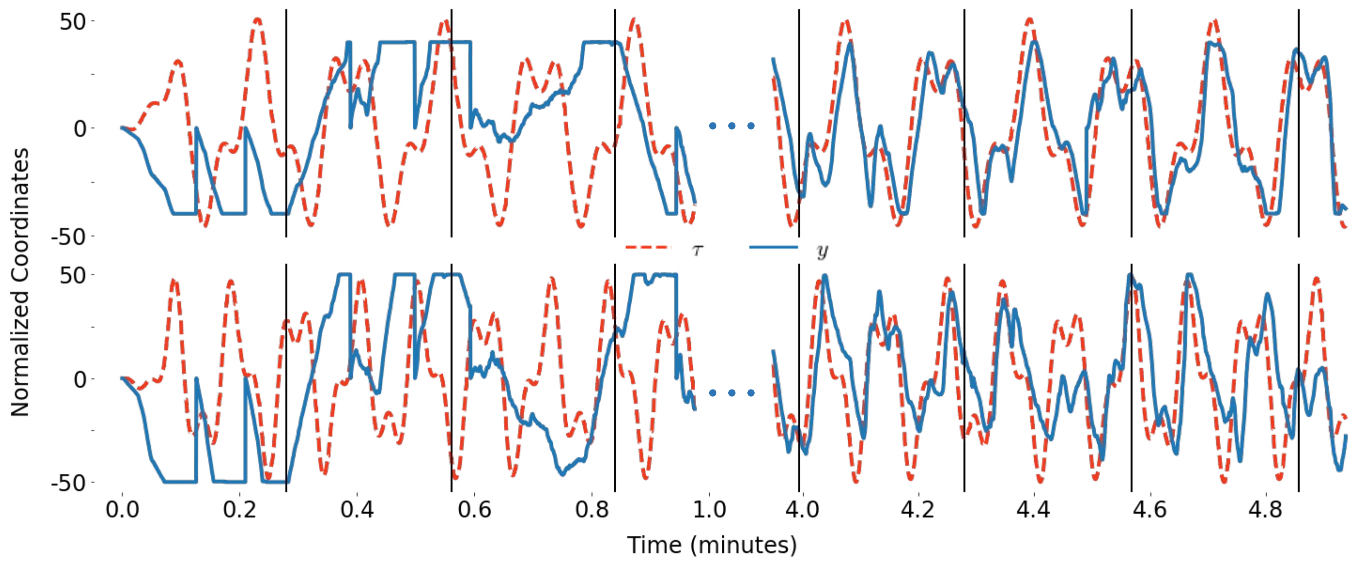

Fig. 2. Comparison of the target (red dashed trace, τ) and cursor (blue straight trace, y) positions over time for one example trial for one subject. The y-axis is normalized coordinates and the x-axis is the time in minutes within the trial. The black vertical lines represent decoder adaptations. Horizontal (x) and vertical (y) positions are shown in the top and bottom plots, respectively.

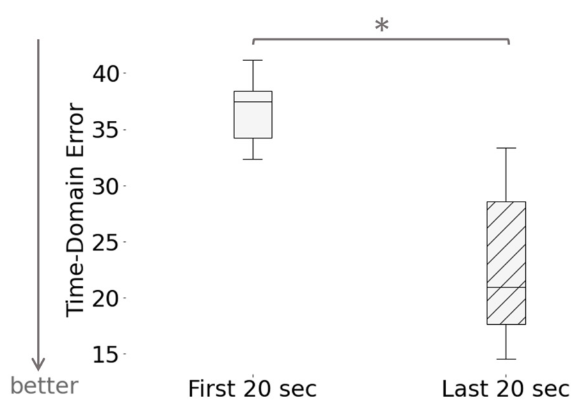

Fig. 3. Time-domain tracking error (Euclidean distance between target and cursor position, $||\tau - y||_2$) averaged over the first 20 seconds and the last 20 seconds. Median error across all conditions (learning rates, decoder initializations, decoder cost weights, blocks) for each subject; statistical comparisons across subjects ($N = 7$) with a Wilcoxon signed-rank test ($p = 0.016$).

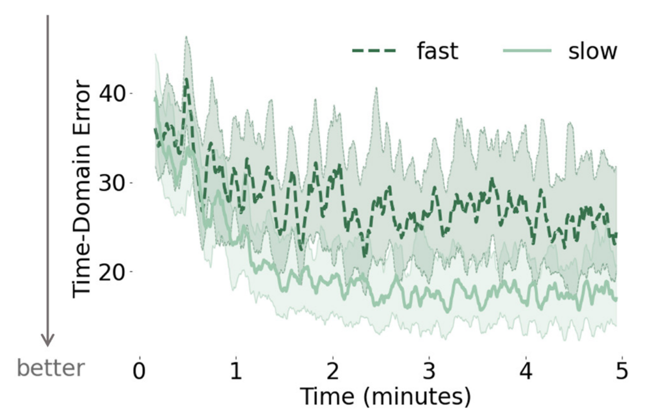

Fig. 4. Median tracking error per subject ($N = 7$) over the five-minute trial, separated by decoder learning rate (slow vs fast). Error was calculated at each timepoint and smoothed with a low-pass filter over 5 seconds for visualization. Solid lines show the median, and shading shows 25% interquartiles.

of the decoder based on the decoder cost weight (Fig. 7). The decoder Frobenius norm is overall higher for the *low* decoder cost weight than for the *high* decoder cost weight.

5. DISCUSSION

This is the first study to test co-adaptive myoelectric interfaces for 2D-continuous control. We observed that updating a randomly-initialized decoder to minimize *task error* and *decoder effort* enabled users to control a 2-dimensional trajectory-tracking task with no calibration. Performance was affected by decoder learning rate but not by initialization nor by cost weights. However, decoder initialization and cost weights influenced the final decoder, suggesting a potential avenue to influence user learning.

In contrast to prior work that optimized exclusively for task error (Orsborn et al., 2012, 2014; Müller et al., 2017) or interaction efficiency (De Santis, 2021), our experiments employed a new decoder adaptation scheme that optimized a cost function that captures the trade-offs of a two-learner human-decoder interface. Similar to previous studies (Orsborn et al., 2012), our co-adaptive framework yielded rapid calibration independent of initialization. But our framework can potentially shape both the decoder *and* the human by changing parameters such as decoder learning rate, initialization, and cost weights.

Similarly to previous studies of learning rate on human-decoder co-adaptation that optimized for task error (Müller et al., 2017), we found that a slow learning rate resulted in a lower task error than a fast learning rate. This may be because slow decoder adaptation is less affected by

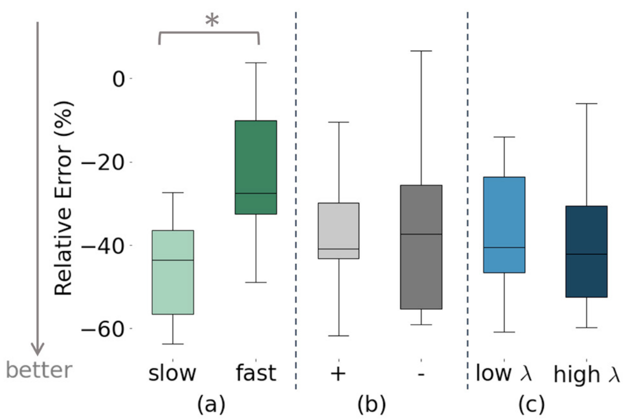

Fig. 5. Median relative error across all blocks and (a) for each learning rates for each subject, (b) for each decoder initialization for each subject, (c) for each decoder cost weight λ for each subject; statistical comparisons across conditions ($N = 7$) with a Wilcoxon signed-rank test ((a) $p = 0.016$, (b) $p = 0.938$, (c) $p = 0.578$). Only (a) is statistically significant ($p < 0.05$)).

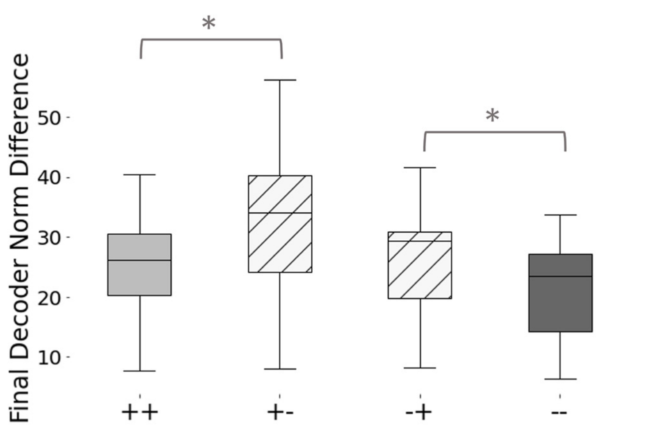

Fig. 6. Sum of squared difference from the group mean for final decoders with either initializations, positive (+) and negative (−), ($||D_{final,avg}$ - $D_{final,subj}||_F^2$). For example, the label +− is $||D_{+,final,avg}$ - $D_{-final,subj}||_F^2$. Statistical comparisons across subjects ($N = 7$) with a paired Wilcoxon signed-rank test. (++ to +−: $p = 0.016$, +− to −+: $p = 0.078$, −+ to −−: $p = 0.016$).

random fluctuations in myoelectric activity or changes in human effort. Performance outcomes could differ with longer trials. Studying variability and performance over longer time scales is important for future work.

Our preliminary analysis suggests that decoder initialization location did not affect task performance, but initialization location did affect the final decoder. The robustness of task performance despite varying decoder initialization locations is congruent with prior co-adaptive algorithms that solely optimized for task performance (Orsborn et al., 2012; Shanechi et al., 2016). Initial performance is a result of the random decoder initialization, so low variance in initial performance across subjects does not reflect sub-

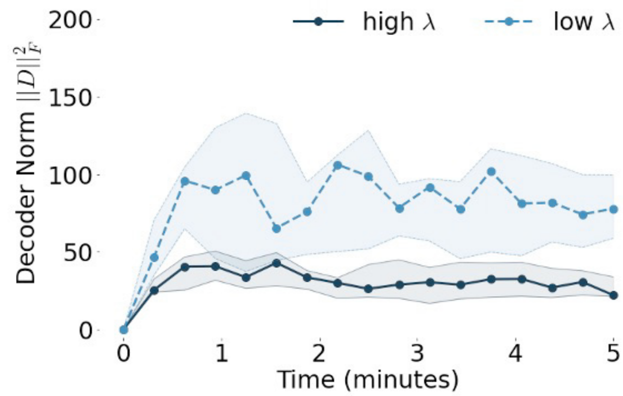

Fig. 7. Decoder norm ($||D||_F^2$) distributions (solid lines show the median, shading shows 25% interquartiles) for median decoder cost weight per subject ($N = 7$) across conditions (blocks, learning rate, decoder initialization). Markers indicate decoder updates.

ject performance. Final performance is due to decoder adaptation and user performance, hence the larger variance across subjects in final versus initial performance. Our finding that the decoder initialization location affects learned decoders is consistent with prior work that theoretically highlighted the existence of multiple equilibria in co-adaptive human-decoder systems (Madduri et al., 2021). In particular, the theoretical analysis in Madduri et al. (2021) suggested that decoder initialization may bias the system towards different equilibria, which we may have observed in this study. Additional analyses and longer-term experiments may help quantify the system equilibria and the effect of decoder initialization location on the final decoder location. We also acknowledge that experiments with a higher number of subjects would be valuable to strengthen these results.

Lastly, our experiments suggest that decoder cost weights influenced the learned decoder without impacting task performance. This finding that a higher decoder cost weight led to a lower decoder Frobenius norm is consistent with theoretical expectations of minimizing the decoder cost. Task performance being unaffected by different decoder norms suggests that users may be able to learn multiple decoders. Users might be potentially compensating for different decoders in their learned strategies. A particularly compelling question for future work is whether the user's encoding or control strategy is biased by the decoder parameters of the learning rate, initialization, and cost weights.

6. CONCLUSION

Designing neural interfaces that can adapt to a wide range of users is key to improving neural interface adoption and usability. Neural interfaces that adapt to individual users and shape user learning through co-adaptation could lead to individualized and robust neural interfaces. We approach the analysis and synthesis of co-adaptive neural interfaces from a game-theoretic perspective that treats the human and decoder as two independent agents in a game. This paper informs an initial exploration of the effect of a game-theoretic adaptive decoder framework and differing parameters on user learning. Our future work plans to further explore the effect of decoder initialization and decoder cost parameters on user encoding and learning.

ACKNOWLEDGEMENTS

We thank our research participants for their time.

REFERENCES

Başar, T. and Olsder, G.J. (1999). *Dynamic noncooperative game theory*. Number 23 in Classics in applied mathematics. SIAM, Philadelphia, 2nd ed edition.

Braun, D.A., Ortega, P.A., and Wolpert, D.M. (2009). Nash equilibria in multi-agent motor interactions. *PLoS computational biology*, 5(8), e1000468.

Carmena, J.M. (2013). Advances in Neuroprosthetic Learning and Control. *PLoS Biology*, 11(5), e1001561. doi:10.1371/journal.pbio.1001561. URL `https://dx.plos.org/10.1371/journal.pbio.1001561`.

De Santis, D. (2021). A framework for optimizing co-adaptation in body-machine interfaces. *Frontiers in Neurorobotics*, 15, 40.

Gilja, V., Nuyujukian, P., Chestek, C.A., Cunningham, J.P., Byron, M.Y., Fan, J.M., Churchland, M.M., Kaufman, M.T., Kao, J.C., Ryu, S.I., et al. (2012). A high-performance neural prosthesis enabled by control algorithm design. *Nature neuroscience*, 15(12), 1752–1757.

Hespanha, J.P. (2017). *Noncooperative Game Theory: An Introduction for Engineers and Computer Scientists*. Princeton University Press.

Hochberg, L.R., Bacher, D., Jarosiewicz, B., Masse, N.Y., Simeral, J.D., Vogel, J., Haddadin, S., Liu, J., Cash, S.S., van der Smagt, P., and Donoghue, J.P. (2012). Reach and grasp by people with tetraplegia using a neurally controlled robotic arm. *Nature*, 485(7398). doi:10.1038/nature11076.

Li, Y., Carboni, G., Gonzalez, F., Campolo, D., and Burdet, E. (2019). Differential game theory for versatile physical human–robot interaction. *Nature Machine Intelligence*, 1(1), 36–43.

Li, Y., Tee, K.P., Yan, R., Chan, W.L., and Wu, Y. (2016). A framework of human–robot coordination based on game theory and policy iteration. *IEEE Transactions on Robotics*, 32(6), 1408–1418.

Madduri, M.M., Burden, S.A., and Orsborn, A.L. (2021). A game-theoretic model for co-adaptive brain-machine interfaces. In *2021 10th International IEEE/EMBS Conference on Neural Engineering (NER)*, 327–330. IEEE.

Monderer, D. and Shapley, L.S. (1996). Potential games. *Games and economic behavior*, 14(1), 124–143.

Müller, J.S., Vidaurre, C., Schreuder, M., Meinecke, F.C., Von Bünau, P., and Müller, K.R. (2017). A mathematical model for the two-learners problem. *Journal of neural engineering*, 14(3), 036005.

Orsborn, A.L., Dangi, S., Moorman, H.G., and Carmena, J.M. (2012). Closed-loop decoder adaptation on intermediate time-scales facilitates rapid bmi performance improvements independent of decoder initialization conditions. *IEEE Transactions on Neural Systems and Rehabilitation Engineering*, 20(4), 468–477.

Orsborn, A.L., Moorman, H.G., Overduin, S.A., Shanechi, M.M., Dimitrov, D.F., and Carmena, J.M. (2014). Closed-loop decoder adaptation shapes neural plasticity for skillful neuroprosthetic control. *Neuron*, 82(6), 1380–1393.

Ratliff, L.J., Burden, S.A., and Sastry, S.S. (2013). Characterization and computation of local Nash equilibria in continuous games. In *2013 51st Annual Allerton Conference on Communication, Control, and Computing (Allerton)*. doi:10.1109/Allerton.2013.6736623.

Reinkensmeyer, D.J., Burdet, E., Casadio, M., Krakauer, J.W., Kwakkel, G., Lang, C.E., Swinnen, S.P., Ward, N.S., and Schweighofer, N. (2016). Computational neurorehabilitation: modeling plasticity and learning to predict recovery. *Journal of neuroengineering and rehabilitation*, 13(1), 1–25.

Shanechi, M.M., Orsborn, A.L., and Carmena, J.M. (2016). Robust brain-machine interface design using optimal feedback control modeling and adaptive point process filtering. *PLoS computational biology*, 12(4), e1004730.

Shanechi, M.M., Orsborn, A.L., Moorman, H.G., Gowda, S., Dangi, S., and Carmena, J.M. (2017). Rapid control and feedback rates enhance neuroprosthetic control. *Nature Communications*, 8(1), 13825. doi:10.1038/ncomms13825. URL `http://www.nature.com/articles/ncomms13825`.

Willett, F.R., Avansino, D.T., Hochberg, L.R., Henderson, J.M., and Shenoy, K.V. (2021). High-performance brain-to-text communication via handwriting. *Nature*, 593(7858).

Wodlinger, B., Downey, J.E., Tyler-Kabara, E.C., Schwartz, A.B., Boninger, M.L., and Collinger, J.L. (2015). Ten-dimensional anthropomorphic arm control in a human brain-machine interface: difficulties, solutions, and limitations. *Journal of neural engineering*, 12(1), 016011. doi:10.1088/1741-2560/12/1/016011.

Yamagami, M., Peters, K.M., Milovanovic, I., Kuang, I., Yang, Z., Lu, N., and Steele, K.M. (2018). Assessment of dry epidermal electrodes for long-term electromyography measurements. *Sensors*, 18(4), 1269.

Yamagami, M., Steele, K.M., and Burden, S.A. (2020). Decoding intent with control theory: comparing muscle versus manual interface performance. In *Proceedings of the 2020 CHI conference on human factors in computing systems*, 1–12.

Zhang, R., Li, F., Zhang, T., Yao, D., and Xu, P. (2020). Subject inefficiency phenomenon of motor imagery brain-computer interface: Influence factors and potential solutions. *Brain Science Advances*, 6. doi:10.26599/BSA.2020.9050021.